Asociación Argentina
de Mecánica Computacional

Mecánica Computacional Vol XXVIII, págs. 1077-1087 (artículo completo)
Cristian García Bauza, Pablo Lotito, Lisandro Parente, Marcelo Vénere (Eds.)
Tandil, Argentina, 3-6 Noviembre 2009

EFFECT OF CRYSTALLOGRAPHIC TEXTURE ON FORMABILITY OF BCC SHEET METALS

M.J. Serenelli, M.A. Bertinetti, J.W. Signorelli

Instituto de Física Rosario, (IFIR-CONICET), Universidad Nacional de Rosario
Bv. 27 de Febrero210b, 2000 Rosario Argentina, http://www.ifir-conicet.gov.ar

Keywords: Formability, BCC sheet, Texture components.

Abstract. The effects of typical orientations observed in cold-rolled BCC sheets (i.e. {001}<110>; {112}<110}; {111}<110>; {111}<112> and {554}<225> texture components) on forming properties are numerically studied. It is shown that not all texture components yield forming limits in the same way: {111}<110> and {111}<112> exhibit higher limit strains than {001}<110> and {112}<110} for non balanced biaxial stretching paths. Higher formability is found for {554}<225> texture component. In addition to anisotropy induced by initial texture and its evolution, it is found that when the orthotropic axes of the texture components are inclined 45° relative to the major stretch direction, the effects on the formability play a non-negligible role. The analyses were performed using the Markciniak-Kuczynski-type approach in conjunction with a self-consistent type polycrystal model (MK-VPSC). Finally, this analysis suggested that texture control may be effective in improving material formability.

1 INTRODUCTION

The plastic deformation of a sheet metal into complex shapes is brought about by the imposition of a combination of stresses. Assessing formability often involves determining the maximum strains that can be attained in metals prior to the onset of necking. The sheet metals, produced by a combination of rolling reductions and annealing, suffer anisotropic effects on their properties. They are caused by either: crystallographic anisotropy produced by a preferential distribution of orientations, microstructural anisotropy due to changes in the dislocation arrays, diminution in the grain size, heterogeneity in the deformation field, etc.. A major concern in the sheet-steel industry is to optimize texture with regard to some application of the sheet, since it is well known that crystallographic texture is the principal cause for the anisotropy of some material properties in metals.

In the FCC metal literature, the effects of typical texture components on formability have been extensively investigated (for instance, see Wu et al., 2004; Yoshida et al., 2007; Signorelli and Bertinetti, 2009; Yoshida et al., 2009). These authors have discussed in detail such effects within a rate-dependent polycrystal-plasticity framework, in conjunction with the M-K approach. On the other hand, in the BCC metal literature, the results of numerous investigations to predict the effects of the typical texture components on the r-value and the yield loci can be found. In order to complement the existing research, we estimate to be of great interest to study the effect of these orientations on forming limits.

The purpose of this work is numerically assessing the influence of crystallographic texture on formability of BCC sheet metals in a practical way. This problem can be expressed in the following terms: which small changes could be made on a material (i.e. a BCC material with a given distribution of orientations) to improve the limit strain behavior under specified deformation paths? In what follows, we try to give a quantitative and qualitative first response to the above questions. In particular, the effects of the observed texture in rolled galvanized steel sheets are studied. The analysis is carried out in terms of the typical rolling texture components that characterize a BCC sheet material: {001}<110>, {112}<110>, {111}<110>, {111}<112> and {554}<225>.

2 CONSTITUTIVE MODEL

To simulate the material response, fully accounting for its heterogeneity and anisotropy, a rate-dependent polycrystalline model is employed. The model starts from the viscoplastic (VP) behavior of single crystal and uses a self-consistent (SC) homogenization scheme for the transition to polycrystal (VPSC) response. The VPSC formulation to model the aggregate behavior is implemented in conjunction with the well-known M-K approach. As it has been originally proposed by Marciniak and Kuczynski, their analysis postulated the existence of a material imperfection such as a groove or a narrow band across the width of the sheet.

A detailed discussion of the integration of the polycrystalline model can be found either in a previous edition of the ENIEF congress (Signorelli, 2006) or in the literature (Signorelli et al., 2009).

3 LIMIT STRAIN FOR IDEAL ORIENTATION TEXTURES

Cold-rolling textures in steels have been typically described in terms of fiber orientations. The relative intensities of textures and its distribution along these fibers can be used to distinguish the material's thermo-mechanical history. These fibers have been referred as the α or RD (rolling direction) fiber and γ or ND (normal direction) fiber. The α and γ fibers run from {001}<110> to {111}<110> along <110>||RD and from {111}<110> to {111}<112> along <111>||ND respectively. Both fiber orientations share the {111}<110> orientation and

are visible in the Euler space in the section $\varphi_2 = 45^o$. Material textures obtained by transformation of austenite to ferrite (hot-rolling) followed by cooling frequently include minor but non negligible rotated cube, rotated Goss and ε–fiber ({554}<225>) orientations. To investigate how these material textures affect formability, we modeled various material textures including different spreads of grain orientations around the ideal orientations, in order to describe actual materials. The procedure used for modeling material textures in the present work is similar to that employed previously by Serenelli et al. (2008). To generate the rotation matrix R we used the angle-axis pair, Θ-U:V:W. For detailed information about how the misorientation can be described mathematically, see Signorelli and Bertinetti, 2009. Briefly, the R matrix is given by:

$$\mathbf{R} = \hat{\mathbf{n}} \otimes \hat{\mathbf{n}} + \left(\mathbf{I} - \hat{\mathbf{n}} \otimes \hat{\mathbf{n}}\right)\cos\Theta + \left(\mathbf{I} \times \hat{\mathbf{n}}\right)\sin\Theta$$

where, $\hat{\mathbf{n}}$ is a unit vector that describes the axis, $\mathbf{I}$ is the second-order identity tensor and ω is the rotation angle around the axis $\hat{\mathbf{n}}$. This axis can be either selected as a random distribution of directions or directly as a random set of vectors. In the first case, the proposed random vector $\hat{\mathbf{n}}$ is chosen with a probability function of the current misorientation angle Θ, in order to guarantee a constant density of directions. The angle Θ was defined in a manner to produce either a Uniform or a Gaussian distribution with a mean value of zero and a standard distribution of θ degrees. Crystal and sample symmetry are imposed in order to obtain a fully orthotropic texture. This procedure is repeated to make a discrete set of 1000 orientations. Figure 1 shows the {110} stereographic pole figures for the five generated materials in the two types of texture distributions: Uniform and Gaussian (referred to as U-set and G-set respectively).

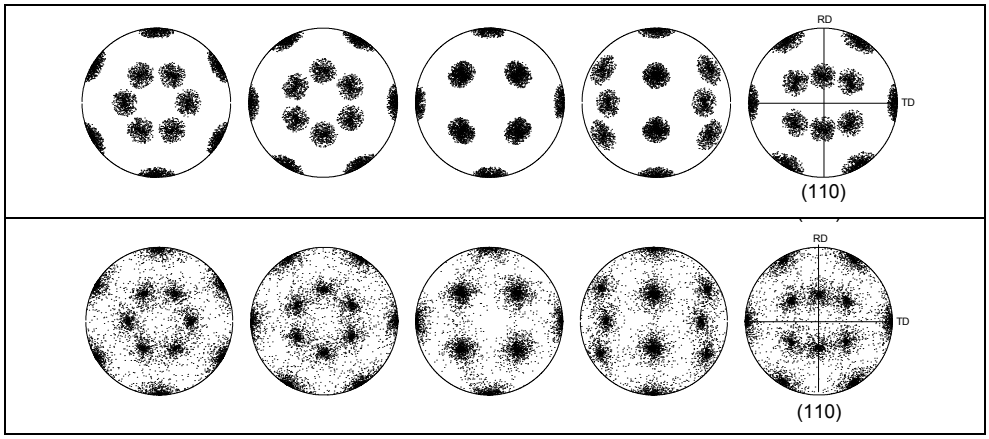

Figure 1: Generated {110} pole figures with 1000 orientations. Top: Uniform distribution with a cut-off angle of 15°. Bottom: Gaussian distribution with a standard deviation of 15°. From left to right: γ_1-texture; γ_2-texture; α_1-texture; α_2-texture and ε-texture.

A cut-off angle of 15° is assumed in the present work, which is the typical value found in the literature. Also, in BCC materials, this value coincides with the maximum misorientation to avoid an overlap between $\alpha_{1\text{-}2}$ fibers and $\gamma_{1\text{-}2}$ fibers. In the case of the ε-fiber, due to the proximity of the γ_2 fiber in Euler space, a misorientation of 15° does not guarantee the absence of an orientation overlap. Table 1 lists the misorientation angles between the ideal orientations described above.

In order to assess the relation between the crystallographic texture developed by the steel sheet and the limit strain values, we analyzed the predicted FLD profiles for the five tested

materials. For all calculations in this work, the values of the material and model parameters are taken from Serenelli et al. (2009). They are: f_0 = 0.995, τ_c = 60MPa, m = 0.02, h_0 = 2.900GPa, n = 0.210 and an aspect ratio of 1:1:0.4.

Ideal orientations	{001}<110>	{112}<110>	{111}<110>	{111}<112>	{554}<225>
{001}<110>	0.0	35.2	54.7	54.7	60.5
{112}<110>	35.2	0.0	19.5	35.6	35.2
{111}<110>	54.7	19.5	0.0	30.0	30.5
{111}<112>	54.7	35.6	30.0	0.0	5.8
{554}<225>	60.5	35.2	30.5	5.8	0.0

Table 1: Misorientation angles in degrees between the five ideal orientations considered here.

Figure 2 shows the predicted FLDs for the five materials of the U-set. The α_1-U exhibits a markedly different material behavior, with a limit-strain curve that slopes downward over the whole right-hand side (RHS) of the forming-limit space. The predicted forming-limits for the other four materials are always greater than the α_1-U limit-strains. Similar values are found for α_2-U, γ_1-U and γ_2-U materials at in-plane plane-strain. Meanwhile, the ε-U material exhibits the highest strain at failure. Another point to note is that α_2-U, γ_2-U and ε-U materials have a maximum limit strain at a plastic strain ratio between 0.3 and 0.4. As these FLDs approach to balanced biaxial tension, ρ = 1, the limit-strain values decrease. The γ_1-U limit strains are relatively constant in the right-hand zone with a maximum value of about 0.3.

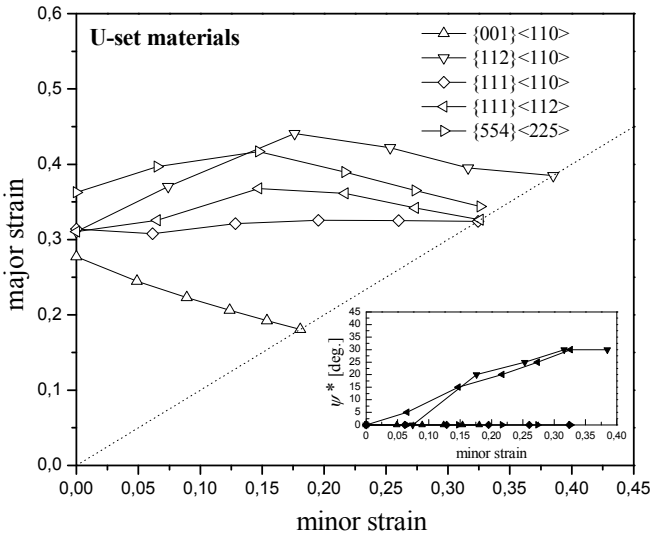

Figure 2: Calculated FLDs assuming a uniform spread distribution with a cut-off angle of 15 degrees.

In a previous work that considered the special case of a FCC material (Signorelli and Bertinetti, 2009), we found that a Gaussian spread of 15 degrees around the ideal {100}<001> orientation would give greater formability and higher limit strains, particularly when the homogenization VPSC scheme is used. To investigate if this effect also takes place for the present materials, we applied a Gaussian distribution of the orientations around the ideal component following the methodology presented above (see section 3 and bottom of the Figure 1). The calculated FLDs for the G-set of materials are displayed in Figure 3. The effects of the distribution type do not modify the global limit-strain behavior with respect to the predictions for the present U-set case. The α_1-G, α_2-G, γ_1-G and γ_2-G materials show very

similar limit-strain profiles, as we predicted for the corresponding U-type cases. Comparing the results of ε-U and ε-G, we can see that the inclusion of non {554}<225> orientations promotes formability for loading paths close to the in-plane plane-strain state, up to ρ = 0.3. For strain ratio values of ρ > 0.3, the calculated major strains are close for both types of orientation distributions.

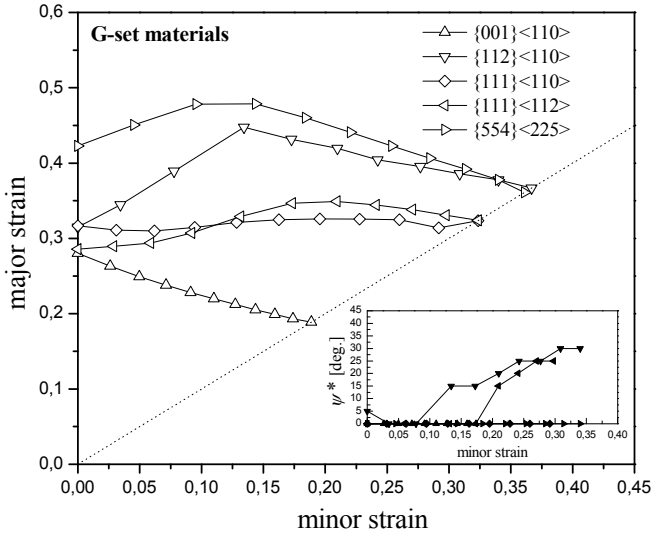

Figure 3: Calculated FLDs assuming a Gaussian spread distribution with a standard deviation of 15 degrees.

Using our simulations, we also studied how texture updating affects the necking limit strain. Previous works (Inal et al, 2005; Tóth et al., 1996) show that the evolution of crystallographic texture has important effects on material failure. We repeated our simulations for ε and γ_2 materials, but without allowing the texture to evolution.

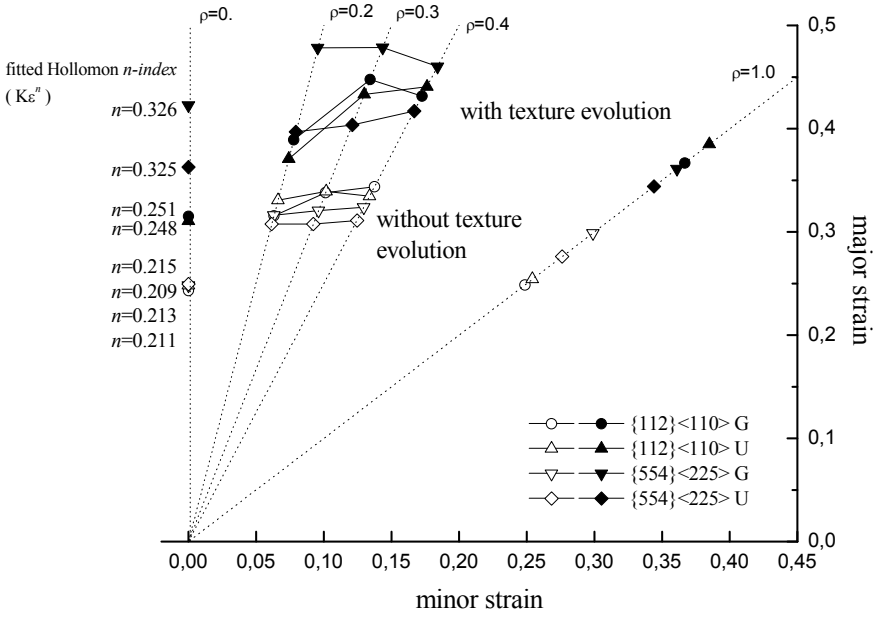

Figure 4: Influence of the texture evolution on the calculated RHS forming-limit strains. With texture evolution (closed symbol), without texture evolution (open symbol).

Clearly, Figure 4 illustrates that texture evolution, hence anisotropy development, produces greater limit strains over the entire RHS of strain space. The predictions, with and without texture evolution, have similar shapes and tendencies over the whole range of ρ values. It is interesting to note that when the texture evolution is turned off, no appreciable differences occur at in-plane plane-strain for the four cases considered. A rapid and frequently diagnosis of sheet-metal forming uses the strain-hardening index n to estimate limit strains along the major strain axis. If we proceed in this way, starting from the VPSC simulated strain-stress tensile curve, we calculate that the values of n are within a narrow range of 0.209-0.215, owing to the slight differences in the calculated limit strains. The validity of this approach was also roughly confirmed when we allowed for texture evolution.

4 STEEL SHEET NECKING ANALYSIS

In this section, two types of results are presented: first, a comparison of an FLD (calculated with the MK-VPSC model with experimental data from a low carbon steel sheet (LCS); secondly, a study of the sensitivity of critical limit strains to a material's texture components.

The initial texture of the steel sheet was measured by X-rays and then from these data an ODF (Orientation Distribution Function) was calculated. As can be seen in Figure 5, the sheet's texture contains slight α–fiber ({001}<110> 1.2%, {112}<110> 9.6%) and a more intense γ–fiber ({111}<110> 18.7%, {111}<112> 9.0%), and {554}<225> 11.7%. The sheet's microstructure is typical of annealed low carbon steels with an ASTM grain size of 6. The ODF was used to generate a set of 1000 grain orientations of appropriate volume fractions. The hardening model and its parameters are given in section 3; the model was calibrated using a uniaxial tension test percent strain. The initial value of the M-K imperfection factor, f_0 = 0.995, was selected in order to obtain the best fit between the simulations and the corresponding experimental data (see Serenelli et al., 2009 for details).

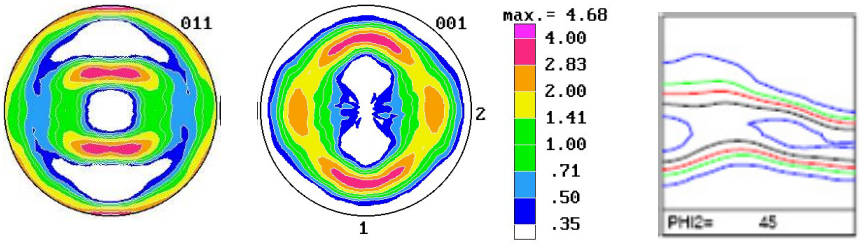

Figure 5: Pole Figures {110}, {200} (contour lines x random) and experimental ODF section 45° (contour lines: 1.00, 2.00, 2.80, 4.00, and 5.60). Frame reference: X_1 top, X_2 right and X_3 centre.

Figure 6 shows a comparison between our predicted FLDs and the experimental limit strains obtained by bulge test with different elliptical masks (Bergé et al., 2008; Serenelli et al., 2009).Two FLD predictions and experiments were made: one when the orthotropic axes of the texture were aligned with the direction of major stretching in the experiments, 0°, and the second when the axes of texture were at 45° to the major stretching direction. As can be seen in Figure 6, the inclination of orthotropic axes had little influence on either the predicted or measured limit strains.

The sheet-steel industry strives to optimize its sheet's formability with the fewest changes possible to the existing processes. Numerically, it is always possible to reduce this problem to an optimal case, where the texture is the variable that minimizes a certain cost function, which describes the difference between the simulated and the target properties. However, this is not

a useful strategy because only narrow changes of the current material texture are feasible within the available processing conditions.

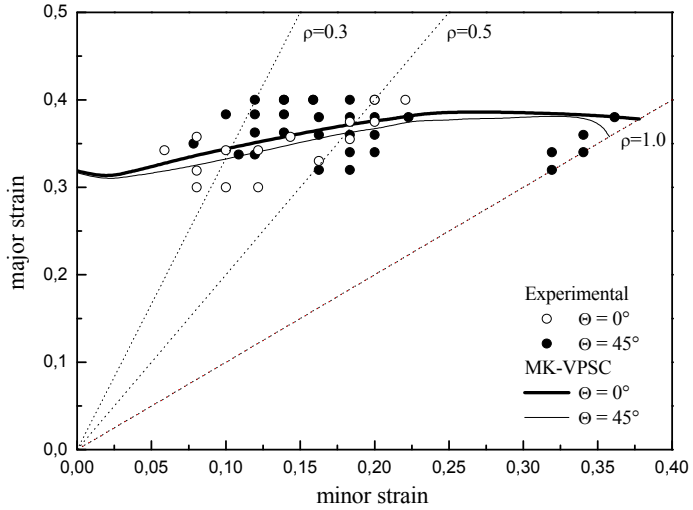

Figure 6: The experimental forming-limit curves with the results of the MK-VPSC simulations. For both, experiment and simulation, the orthotropic axes of the texture components are inclined 0° or 45° relative to the major stretch direction.

In the following, we analyze the sensitivity of the model with respect to a perturbation of the main texture components. Although numerical techniques exist to achieve that purpose, they typically include the calculation of the study variables as derived from the model. Because of this and the difficulty of obtaining such derivatives for the present model, we use a simple inspection method to estimate the sensitivity of the limit-strain to the initial distribution of orientations in the sheet. The methodology used consists of systematically increasing the volume fraction of a given component from its initial value by factors of x0, x2, x5, x10, x25 and x50 (i.e., the initial volume fraction of the orientation(s) that belong(s) to a given component are increased proportionally, then all sets of orientation weights are renormalized in order to ensure that the sum of all volume fractions remains equal to the initial value).

Figure 7 shows the simulation performed for each of the five components analyzed. Included in the figure are the LCS sheet's FLDs and the ideal components (α_1-U, α_2-U, γ_1-U, γ_2-U and ε-U). Due a matter of clarity, only the FLDs corresponding to factors of x0, x10 and x50 are plotted. From these figures, it is clear that the limit strains depend only slightly on the intensity of the α_1, α_2, γ_1 or γ_2 orientations for in-plane plane-strain. Only when we considered ε-type orientations did we find an appreciable variation in limit strains. This is in agreement with the analysis presented previously in section 3. For $\rho > 0$ the material sensitivity generally increases: α_1, γ_1, and γ_2 texture components show a tendency to decrease the limit strain as their presences increase in the material texture; α_2 promotes an increase in the deformation to failure for loads around $\rho = 0.5$, although its effects decreases as we approach equi-biaxial stretching.

In what follows, we highlight some of the more outstanding aspects observed in the calculated sensitivity-profile of each component:

- {001}<110>: the presence of this component causes a decrease in the exhibited limit-strains. The rate of these changes varies with the applied stretching paths. The more pronounced changes take place for $\rho > 0.5$, while at in-plane plane-strain, the strain

limit response is almost insensitive up to volume fractions of 25-30% for {001}<110> orientations.

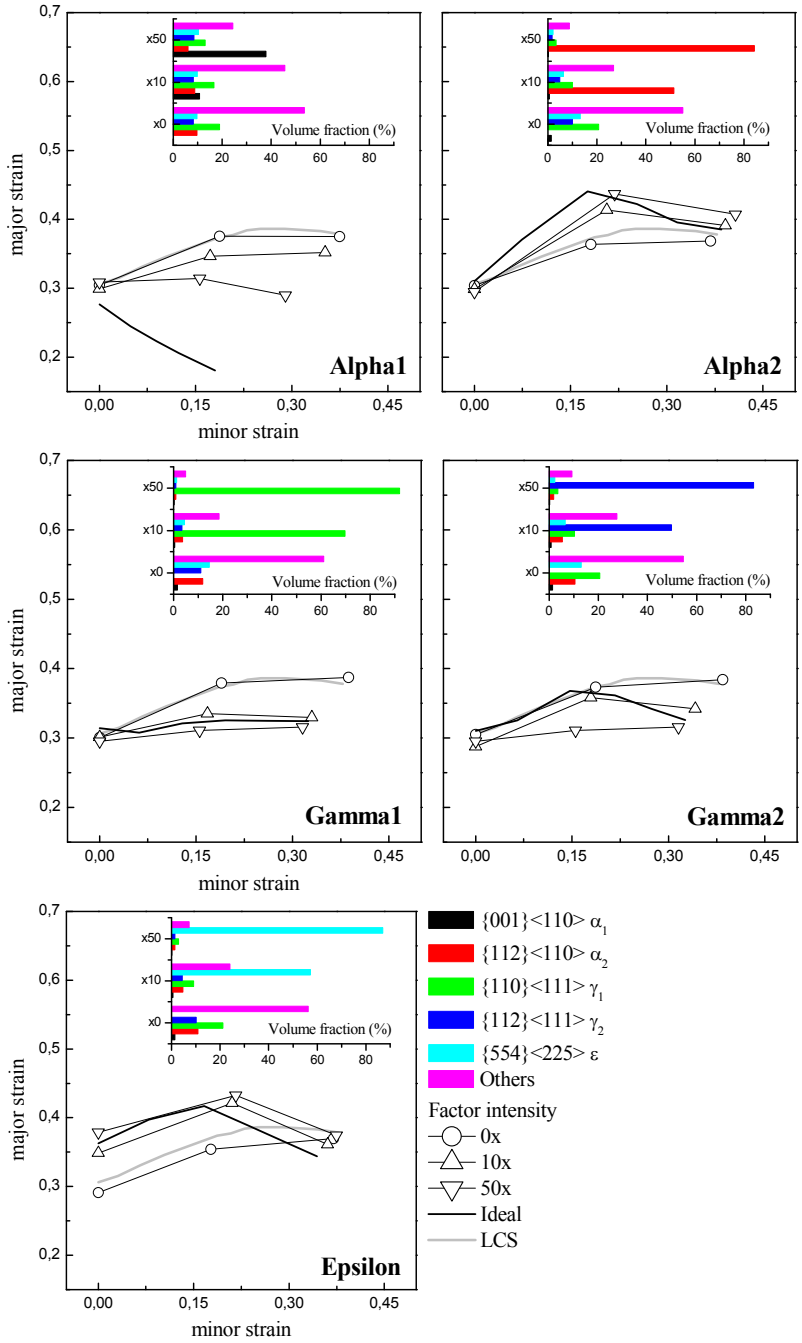

Figure 7: Sensitivity analysis of the forming-limit behavior for each component analyzed.

- {112}<110>: similarly to {001}<110>, this component has the maximum limit-strain value close to ρ = 0.5. But, in opposite to {001}<110>, the tendency is quite different at equi-biaxial stretching. A nearly constant behavior is observed when the volume fraction reaches values up to 60-70%, meanwhile for in-plane plane-strain, the limit-strains values slightly diminish with an increase of the volume fraction.
- {111}<110> - {111}<121>: both components show a relative similar behavior. The formability decreases as the volume fraction of gamma orientations increases. No

appreciable differences can be found for ρ > 0.4 - 0.5. Moreover, minor differences are predicted for ρ = 0.0.

- {554}<225>: this orientation has a particular interest in our analysis since it is the only one that shows a clear sensitivity under plane-strain condition. Normally, for ρ = 0.0, BCC steel sheets show a minimum value for the major strain. In principe, it could be possible to obtain higher limit-strains by increasing this component´s volume fraction, although in a small quantity. This behavior is observed for low and intermediate values of volume fraction (up to 0.40). For higher volume fractions, the limit strains only show minor changes. Note that cold-rolling steel sheets always show much less volume fraction of this type of orientations.

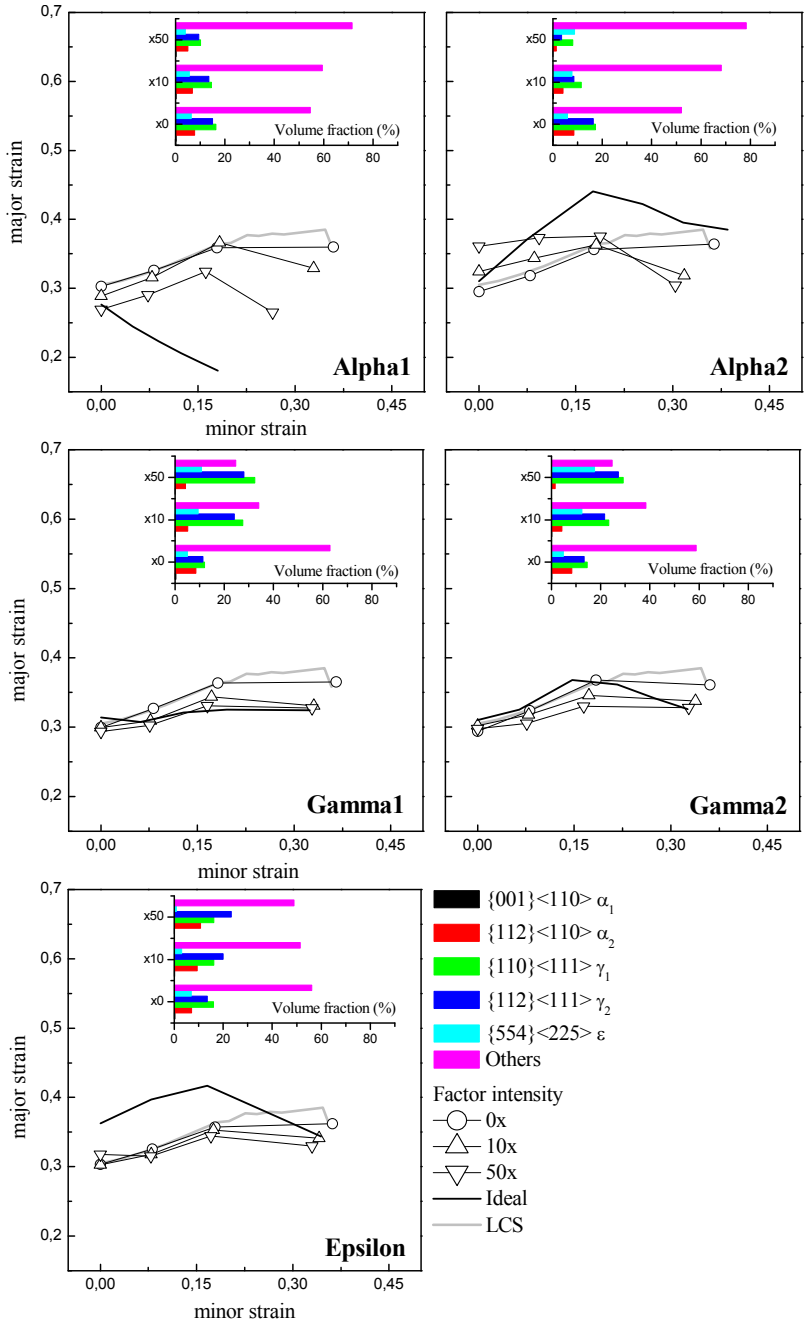

Figure 8: Sensitivity analysis of the forming-limit behavior for a rotation of θ = 45˚ of the major stretching direction relative to the orthotropic axes of the texture, for each component analyzed.

In Figure 8, we analyze the effects of texture on the limit-strain values when the major stretching direction is rotated 45˚ relative to the orthotropic axes of texture. For this configuration, changes are almost negligible for the α_1-type component. The gamma fiber (γ_1 and γ_2) also shows the same forming limits as those predicted for $\theta = 0^\circ$. But, unlike the previous case, this result can be explained in terms of the rotated textures. As can be seen in the details of this figure, when the original γ_1 / γ_2 orientations are rotated, in each γ-type orientation it is verified that the sums of γ_1 and γ_2 volume fractions are the same, and equal to the original γ_1 / γ_2 orientations (see green and blue bars in the details Gamma1 and Gamma2 in Figure 8). The presence of a higher gamma fiber gives a more 'isotropic' response respect to a change in the inclination in relation to the major-stretch direction, where 'isotropy' refers to a smaller influence of the inclination between the orthotropic axes and the principal strains on formability. Close to the equi-biaxial stretching zone, an increase in its volume fraction causes a slight increment on the limit-strains. Forming limits for ε-type orientations with $\theta = 0^\circ$ are significantly affected when inclined $\theta = 45^\circ$. While the ε-type orientations exhibit higher limit-strains for $\theta = 0^\circ$, the enhancing of formability is transferred to the α_2-type orientation for $\theta = 45^\circ$.

5 CONCLUSIONS

In the present study, the sensitivity of the formability to changes in texture for BCC steel sheets has been systematically investigated, under biaxial stretching mode, using a self-consistent viscoplastic polycrystalline model.

It is observed that texture evolution produces greater limit strains over the entire RHS of strain space for the five analyzed material textures. We find that, for in-plane plane-strain, the forming limits are almost insensitive to relative changes of α_1, α_2, γ_1, γ_2 material textures; but for ε-type orientations positive variations in the limit-strain values are clearly observed. For $\rho > 0$, the material sensitivity generally increases for α_1 and γ_1, while γ_2 shows a tendency to decrease the limit strain as its volume fraction grows.

For $\theta = 45°$, and compared with $\theta = 0^\circ$, minimal variations can be appreciated on the predicted limit strains for the gamma-orientations. Also, higher variation in the forming-limit values for $\rho = 0$ is transferred from ε-type to α_2-type orientations.

The simulations clearly show that an increase on formability can be obtained via the control of the texture, enhancing the geometrical hardening. The theoretically computed critical-strains show an expected behavior in both, in-plane plane-strain and biaxial stretching. Taking into account that all these calculations are computational results, associated with a specific homogenization model and, as is known that the forming limits strongly depend on the selected homogenization method, experimental research should be carried out to validate them. A first attempt can be found in Serenelli et al. (2009).

REFERENCES

Bergé, G., Puccinelli, M., Insausti, J., Ziegler, D., Lucaioli, A. y Iurman, L. Influencia de la anisotropía planar en la trayectoria de deformación de una chapa de acero electrocincada bajo tracción biaxial no equilibrada, *Proceedings Congreso SAM-CONAMET 2008*, en edición.

Inal, K., Neale, K., Aboutajeddine, A. Forming limit comparison for FCC and BCC sheets, *International Journal of Plasticity*, 21:1255–66, 2005.

Serenelli, M., Bertinetti, M.A. y Signorelli, J. Influencia de la textura cristalográfica en la dispersión de coeficientes de Lankford en una chapa de acero galvanizada de bajo carbono,

Mecánica Computacional Vol. XXVII, 993-1002, 2008.

Serenelli, M., Bertinetti, M.A., Insausti, J., Lucaioli, A., Ziegler, D., y Signorelli, J. Modelización de las deformaciones límite de una chapa de acero electrocincada bajo tracción biaxial, *Proceedings Congreso SAM-CONAMET 2009*, en edición.

Signorelli, J.W. Predicción de la curva límite de formabilidad utilizando un modelo autoconsistente viscoplástico, *Mecánica Computacional Vol. XXV*, 2082-2096, 2006.

Signorelli, J.W. and Bertinetti, M.A. On the role of constitutive model in the forming limit of FCC sheet metal with cube orientations, *International Journal of Mechanical Sciences*, 51: 473-480, 2009.

Signorelli, J.W., Bertinetti M.A., Turner P.A. Predictions of forming limit diagrams using a rate-dependent polycrystal self-consistent plasticity model, *International Journal of Plasticity*, 25:1-25, 2009.

Toth, L., Dudzinski, D., Molinari, A. Forming limit predictions with the perturbation method using stress potential functions of polycrystal viscoplasticity. *International Journal of Mechanical Sciences*, 38: 805–824, 1996.

Wu, P.D., MacEwen, S.R., Lloyd, D.J and Neale, K.W. Effect of Cube Texture on Sheet Metal Formability, *Materials Science and Engineering A*, 364:182-187, 2004.

Yoshida, K., Ishizaka, T., Kuroda M. and Ikawa, S. The Effects of Texture on Formability of Aluminum Alloy Sheets, *Acta Materialia* 55:4499-4506, 2007.

Yoshida, K., Tadano, K. and Kuroda M. Improvement in formability of aluminum alloy sheet by enhancing geometrical hardening, *Computational Material Science* 46:459-468, 2009.